



Enhanced magneto-optical Kerr effect in oxidized Co thin films

B. Rellinghaus, S. Fernandez de Avila, D. Weller, G. Armelles, R. Beyers et al.

Citation: *J. Appl. Phys.* **83**, 5621 (1998); doi: 10.1063/1.367413

View online: <http://dx.doi.org/10.1063/1.367413>

View Table of Contents: <http://jap.aip.org/resource/1/JAPIAU/v83/i11>

Published by the [American Institute of Physics](http://www.aip.org).

Related Articles

Optical properties and electronic structure of multiferroic hexagonal orthoferrites RFeO₃ (R=Ho, Er, Lu)
J. Appl. Phys. **111**, 056105 (2012)

Bulk-like dielectric properties from metallo-organic solution-deposited SrTiO₃ films on Pt-coated Si substrates
J. Appl. Phys. **111**, 054108 (2012)

Optical properties of amorphous high-k LaGdO₃ films and its band alignment with Si
J. Appl. Phys. **111**, 044106 (2012)

Characterization of silicon dioxide films on 4H-SiC Si (0001) face by cathodoluminescence spectroscopy and x-ray photoelectron spectroscopy
Appl. Phys. Lett. **100**, 082105 (2012)

The absorption property of single crystal LuBiIG garnet film in terahertz band
J. Appl. Phys. **111**, 07A513 (2012)

Additional information on *J. Appl. Phys.*

Journal Homepage: <http://jap.aip.org/>

Journal Information: http://jap.aip.org/about/about_the_journal

Top downloads: http://jap.aip.org/features/most_downloaded

Information for Authors: <http://jap.aip.org/authors>

ADVERTISEMENT



**FIND THE NEEDLE IN THE
HIRING HAYSTACK**

Post jobs and reach
thousands of hard-to-find
scientists with specific skills



<http://careers.physicstoday.org/post.cfm> **physicstoday** JOBS

Enhanced magneto-optical Kerr effect in oxidized Co thin films

B. Rellinghaus,^{a)} S. Fernandez de Avila,^{b)} D. Weller, G. Armelles,^{c)} R. Beyers,
and A. Kellock

IBM Research Division, Almaden Research Center, San Jose, California 95120-6099

(Received 1 December 1997; accepted for publication 18 February 1998)

We have studied the structural and magneto-optical properties of postdeposition oxidized Co thin films. The oxidization process leads to the formation of a double-layered structure of fcc Co_3O_4 on top of metallic Co. The magneto-optical Kerr effect (MOKE), measured in the range $0.8 \text{ eV} \leq E_{\text{ph}} \leq 5.5 \text{ eV}$ reveals characteristic dependencies of the MOKE spectra on annealing temperature and time. In particular, we observe resonance-type enhancements of the Kerr effects by up to a factor of 10 compared with unannealed metallic Co. The experimental data are quantitatively reproduced by bilayer optical stack calculations. © 1998 American Institute of Physics. [S0021-8979(98)06510-4]

I. INTRODUCTION

Multilayered (ML) structures consisting of alternating nonmagnetic and magneto-optically active layers are of significant importance in the field of magneto-optical (MO) recording.¹⁻⁴ In these ML systems, the magneto-optical Kerr effect (MOKE) can be strongly enhanced due to the optical properties of the nonmagnetic spacer layers. E.g., in Fe/Cu bilayered films, the Kerr rotation Θ_K was found to increase strongly in the energetic vicinity of the plasma edge of the underlying Cu layer.⁴ Enhancements of this type have been suggested to improve the read-back signal of magneto-optical recording media.⁵

In the present paper we discuss the possibility of modifying the magneto-optical properties of polycrystalline Co films by postdeposition annealing in air or oxygen. We show that ‘‘natural’’ oxide layers form on top of metallic Co leading to magneto-optically active bilayers. Such postdeposition processing could become technologically relevant. In order to investigate the magneto-optical properties of these oxide/Co bilayered films we have measured the polar magneto-optical Kerr effect in the photon energy range $0.8 \text{ eV} \leq E_{\text{ph}} \leq 5.5 \text{ eV}$.

II. SAMPLE PREPARATION AND CHARACTERIZATION

The present Co films were prepared by dc magnetron sputtering at room temperature or electron-beam evaporation (EBE) at $T_g \approx 190 \text{ }^\circ\text{C}$. For the sputtering process, pure Ar at pressures $1 \text{ mbar} \leq p \leq 10 \text{ mbar}$ has been used as the sputter gas. Growth rates have been varied between 0.04 and $0.5 \text{ } \text{Å s}^{-1}$. Electron-beam evaporation has been carried out in a $p_{\text{base}} \approx 5 \times 10^{-9} \text{ mbar}$ base pressure system. The pressure

during deposition was $5 \times 10^{-7} \text{ mbar} \leq p \leq 5 \times 10^{-8} \text{ mbar}$ and typical growth rates were $0.1 \text{ } \text{Å s}^{-1} \leq r \leq 0.2 \text{ } \text{Å s}^{-1}$. Substrates were fused silica (quartz), Si, or SiN_x -coated Si.

After the deposition the films were subjected to various annealing procedures. The samples were exposed to air or oxygen at temperatures $150 \text{ }^\circ\text{C} \leq T_{\text{ann}} \leq 350 \text{ }^\circ\text{C}$ for annealing times $1 \text{ h} \leq \tau_{\text{ann}} \leq 10 \text{ h}$.

Structural and compositional characterization of the samples has been carried out using transmission electron microscopy (TEM), Rutherford backscattering spectrometry (RBS), and x-ray diffraction (XRD). Figure 1(a) shows, as an example, a cross-sectional TEM image of a $2500 \text{ } \text{Å}$ thick Co film, which has been electron-beam evaporated at $T_g = 190 \text{ }^\circ\text{C}$ on a $400 \text{ } \text{Å}$ SiN_x -coated Si substrate which was preseeded with $100 \text{ } \text{Å}$ Pt. The sample was annealed for 1 h at $T_{\text{ann}} = 280 \text{ }^\circ\text{C}$ in oxygen. The film consists of two layers: $1800 \text{ } \text{Å}$ of metallic Co covered with a well-separated $1100 \text{ } \text{Å}$ thick oxide layer. From a Fourier transform analysis of the top layer in the TEM bright-field image (cf. Fig. 2), as well as from RBS and XRD investigations, the oxide is determined to be fcc Co_3O_4 . From the Θ - 2Θ XRD scan of the sample shown in Fig. 2 one can see that the metallic Co layer consists of both hexagonal and fcc regions. Additional TEM investigations reveal that the hexagonal structure is the predominant phase coexisting with minor fcc regions in this Co layer.

The total film thickness as taken from the TEM image ($t_{\text{ann}} = 2900 \text{ } \text{Å}$) is found to be significantly larger than the nominal thickness of the unoxidized Co film ($t = 2500 \text{ } \text{Å}$). This discrepancy is attributed to the incorporation of oxygen during the oxidization process leading to a brittle surface oxide with reduced density. [cf. Fig. 1(a)].

Figure 1(b) shows a cross-sectional TEM image of an ‘‘as-deposited’’ film of $100 \text{ } \text{Å}$ Co sputtered on Si/400 Å SiN_x at room temperature (RT) at $p = 6 \text{ mbar}$ Ar gas pressure. This sample has not been subjected to any annealing procedure, and though it is harder to see from the TEM image, it also exhibits a similar double-layered structure of a thin oxide layer on top of the unoxidized metallic Co. This is

^{a)}Permanent address: Gerhard-Mercator-Universität Duisburg, Experimentelle Tieftemperaturphysik, Lotharstrasse 1, 47048 Duisburg, FRG. Electronic mail: brell@tphysik.Uni-Duisburg.DE

^{b)}Permanent address: Universidad Alfonso X ‘‘El Sabio,’’ Desp. 285, Dept. Matemáticas y Física Aplicada, Avenida de la Casquada Madrid 28691, Spain.

^{c)}Permanent address: Instituto de Microelectronica de Madrid Isaac Newton 8 (PTM), Tres Cantos Madrid 28760-E, Spain.

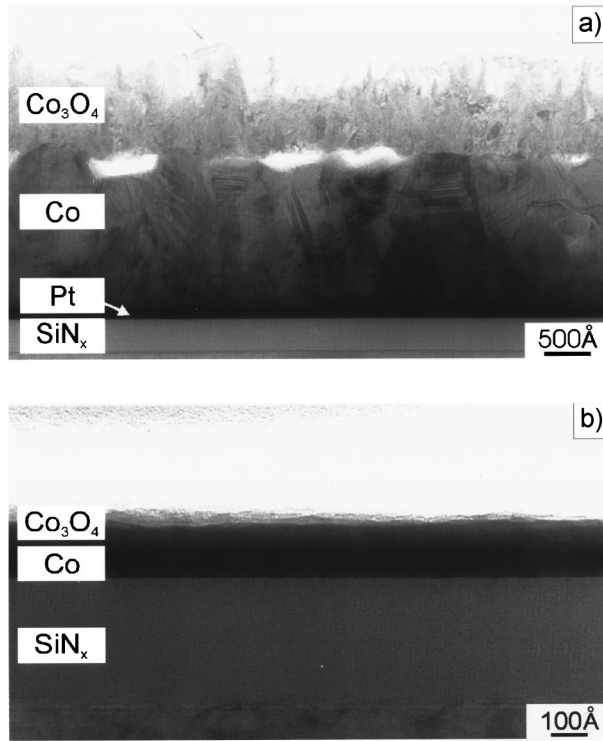


FIG. 1. TEM cross section images of (a) 2500 Å Co evaporated on Si/400 Å SiN_x/100 Å Pt at $T_g = 190^\circ\text{C}$ and subsequently oxygen annealed for 1 h at $T_{\text{ann}} = 280^\circ\text{C}$, and (b) 100 Å Co sputtered on Si/400 Å SiN_x at $T_g = \text{RT}$.

simply due to air oxidation at room temperature prior to the TEM investigations.

III. MAGNETO-OPTICAL PROPERTIES

To study the effect of annealing in air or oxygen on the magneto-optical properties of thin Co films we have prepared a variety of samples under different growth conditions. In the present paper we show the results of investigations on a series of 1000 Å thick Co films sputtered on fused silica substrates at an Ar pressure of $p = 3$ mbar at RT. The samples were annealed in air for different times τ_{ann} and

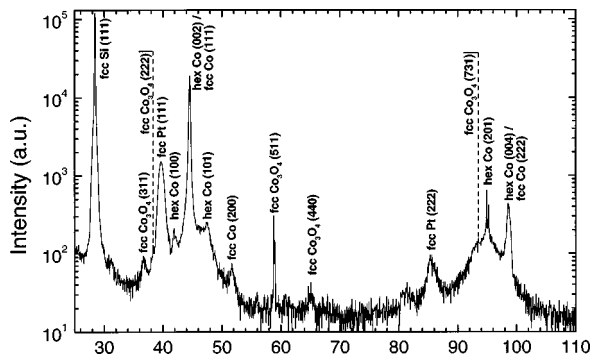


FIG. 2. Θ - 2Θ XRD scan of 2500 Å Co evaporated on Si/400 Å SiN_x/100 Å Pt at $T_g = 190^\circ\text{C}$ and subsequently oxygen annealed for 1 h at $T_{\text{ann}} = 280^\circ\text{C}$ (cf. Fig. 1). The intensity is given on a logarithmic scale as function of 2Θ . The Si and Pt peaks originate from the substrate and seed layer, respectively.

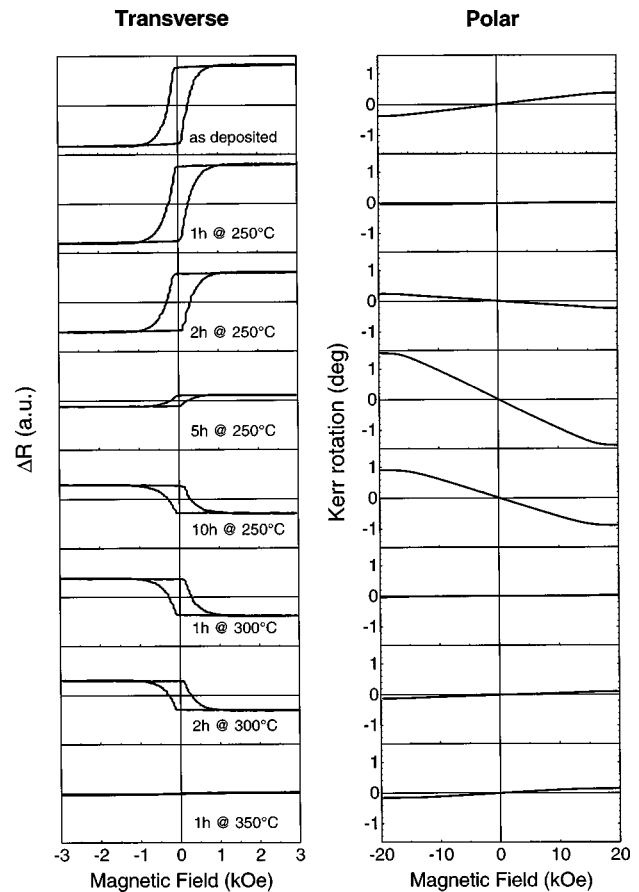


FIG. 3. Transverse (left column) and polar (right column) Kerr loops of a series of 1000 Å thick Co films after being subjected to various annealing procedures in air. Note the different field scales at the transverse and polar loops, respectively.

temperatures T_{ann} : 1 h at 250°C , 2 h at 250°C , 5 h at 250°C , 10 h at 250°C , 1 h at 300°C , 2 h at 300°C , and 1 h at 350°C . Samples being annealed at temperatures $T_{\text{ann}} < 250^\circ\text{C}$ are omitted here, since only minor changes in their magneto-optical properties were detected. We point out that the results presented here are characteristic for a broad spectrum of preparation parameters. Changing, e.g., the substrate, the preparation method (EBE/sputtering), the growth temperature, or the annealing atmosphere (air/oxygen) did *not* significantly influence the magneto-optical properties of the films. Annealing temperature and time, on the other hand, turned out to be key parameters controlling both the structure and magneto-optics of these samples.

Figure 3 shows the transverse (left column) and polar (right column) Kerr hysteresis loops for the seven samples of the above series. The measurements have been performed at RT using a 633 nm HeNe laser (photon energy $E_{\text{ph}} = 1.96$ eV). In the transverse configuration, where the magnetic field is parallel to the sample plane, the measured change in the reflection coefficients of s and p polarized waves ΔR is proportional to the component of the magnetization within the film plane. In the polar configuration the field is applied parallel to the film normal, and the measured Kerr rotation is proportional to the out-of-plane component of the magnetization. It can be seen from Fig. 3 that the easy

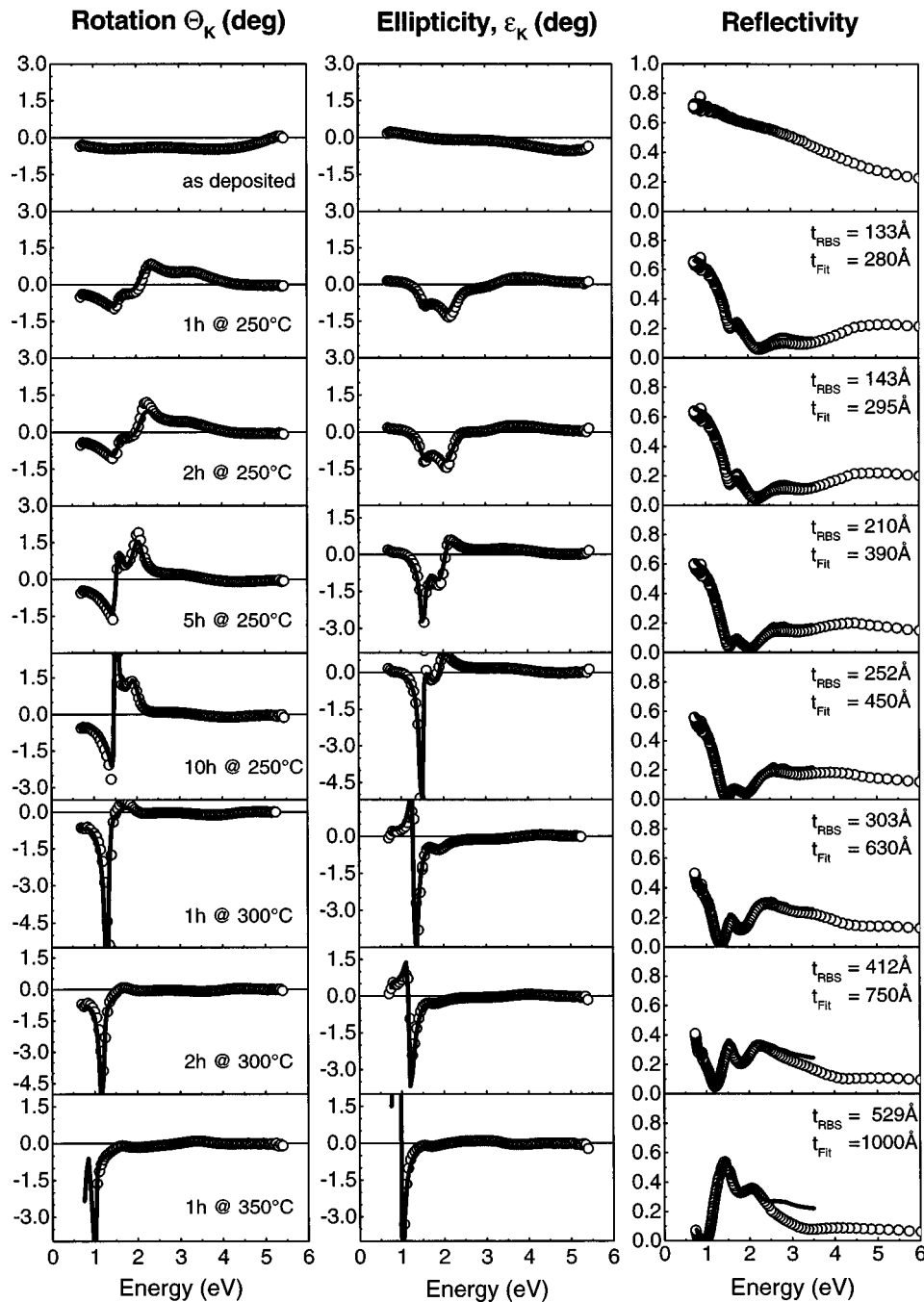


FIG. 4. Complex polar MOKE spectra and reflectivity at normal incidence R of 1000 \AA thick Co films after different degrees of annealing: Kerr rotation (left column), Θ_K , ellipticity (midcolumn), ϵ_K , and reflectivity (right column) as functions of the photon energy. The open circles denote the experimental results, whereas the solid lines represent the result of bilayer optical stack calculations. The thicknesses of the oxide layers as determined from RBS experiments, t_{RBS} , and as fitted within the model calculations, t_{Fit} , are also given.

axis of magnetization lies within the plane, as is expected for these film thicknesses.⁶⁻⁸ Neither the coercivity as taken from the easy-axis loops (transverse configuration) nor the hard-axis saturation fields obtained from the polar loops undergo significant changes, although the magnitude and sign of the MOKE signals vary strongly with an increasing degree of annealing. Since Co_3O_4 is paramagnetic at RT (Ref. 9) [like all oxides of Co (Ref. 10)], this lends support to the assumption that the *magneto*-optic response of the samples originates from the unaltered metallic Co underneath the oxidized top layer. Thus, the measured hysteresis loops are con-

sistent with the results of the structural investigations.

Polar MOKE spectral dependencies were measured in the photon energy range $0.8 \text{ eV} \leq E_{\text{ph}} \leq 5.5 \text{ eV}$ using a fully automated spectrometer based on a zeroing technique.¹¹ Figure 4 shows complex MOKE spectra [Kerr rotation Θ_K (left column) and ellipticity ϵ_K (right column)] for all samples of the present series. For the “as-deposited” film, $\Theta_K(E_{\text{ph}})$ and $\epsilon_K(E_{\text{ph}})$ show relatively weak energy dependencies and are comparable to previously published spectra for hexagonal Co.¹² Air annealing leads to distinct resonance-type features in both Θ_K and ϵ_K . With an increasing degree of annealing

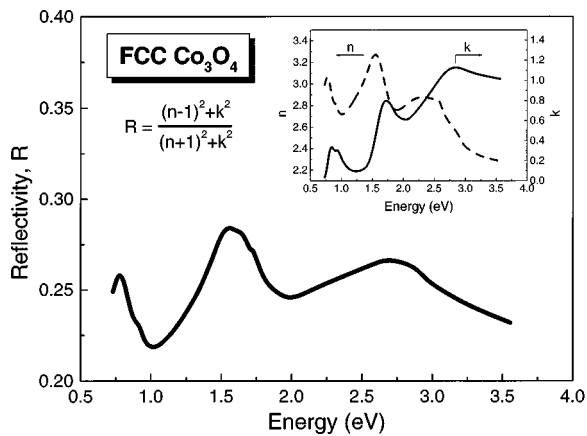


FIG. 5. Energy dependence of the reflectivity R for fcc Co_3O_4 as calculated from the optical constants after Ruzakowski Athey *et al.* (Ref. 13). The spectral dependences of n and k are shown in the inset.

(i.e., increasing T_{ann} and/or τ_{ann}), these resonances are shifted towards lower energies (*redshift*) and grow in magnitude. Peak Kerr rotations of up to $\Theta_K = -5.5^\circ$ at $E_{\text{ph}} \approx 1.3$ eV for the sample annealed for 1 h at $T_{\text{ann}} = 300^\circ\text{C}$ are obtained. To investigate the origin of these enhancement effects we have also measured the energy dependence of the reflectivity at normal incidence R . The results are shown in the right column of Fig. 4. A strong reduction of R over a broad energy range and the development of two local minima with the increasing degree of annealing is observed. It is obvious that the extrema in $\Theta_K(E_{\text{ph}})$ coincide with the minima in $R(E_{\text{ph}})$, the latter being directly related to the (effective) optical constants of the films.¹¹

The spectral dependence of the optical constants of fcc Co_3O_4 in the energy range $0.7 \text{ eV} \leq E_{\text{ph}} \leq 3.5 \text{ eV}$ has been published recently.¹³ The data show spectral features correlating with those in the MOKE spectra of our air-annealed Co films. In particular, the extinction coefficient k drops almost to zero near $E_{\text{ph}} \approx 1.2$ eV, which is the range of strongest MOKE enhancement. In Fig. 5 we show the energy dependence of the reflectivity of fcc Co_3O_4 as calculated from the n and k data after Ruzakowski Athey *et al.*¹³ (cf. inset in Fig. 5). The qualitative agreement between the spectral dependence of the reflectivity for fcc Co_3O_4 on the one side and for our air-annealed Co films on the other side indicates that the present enhancement effects have their origin in the optical properties of the oxide layer. This assumption can be directly verified by using bilayer optical stack calculations. We have performed such calculations using the published optical constants of (nonmagnetic) fcc Co_3O_4 (Ref. 13) and an optical stack code based on Yeh's 4×4 matrix formalism.¹⁴ Input data for the metallic Co layer were published optical constants¹⁵ and measured $\Theta_K(E_{\text{ph}})$ and $\epsilon_K(E_{\text{ph}})$ spectra from a thick "as-deposited" Co film. In these model calculations one assumes optically flat interfaces between the various layers, and quantitative agreement with the experiment may be expected to the extent that this condition as well as the input parameters are correct. The thickness of the Co layer is set to the values determined from the RBS experiments. The thickness of the oxide layer is also

initially set to the RBS value, however, then varied iteratively until a best fit with the experimental data is reached.

The results of these model calculations are included as solid lines in Fig. 4. As can be seen, we obtain good agreement with the experimental data. Only for the samples with the highest degree of annealing (2 h at 300°C and 1 h at 350°C), the calculated reflectivity deviates from the measured data at energies $E_{\text{ph}} \geq 2.5$ eV. This, we think, is attributable to a relatively large roughnesses of up to $\Delta t_{\text{ox}} \approx 500 \text{ \AA}$ in these samples as determined by atomic force microscopy.

The fitted oxide layer thicknesses t_{Fit} can be compared with the respective RBS thicknesses t_{RBS} , which we have done in Fig. 4. We find it interesting to note that there is a significant discrepancy between t_{RBS} and t_{Fit} for all samples of the present series. This can be attributed to porosities in the Co-oxide layers as, e.g., evident in the TEM images. Such porosities are picked up in the optical method, which measures an oxide thickness consistent with the value extracted, e.g., from TEM. However, they are neglected in the RBS analysis, which assumes bulk density. As an example, we find $t_{\text{Fit}} = 1100 \text{ \AA}$ for the film depicted in Fig. 1(a) by utilizing the bilayer optical stack model, which is in good agreement with the actual thickness taken from the TEM image.

IV. CONCLUSION

We have investigated the structural and magneto-optical properties of oxidized Co films. From TEM, XRD, and RBS experiments the postdeposition oxidation process is found to result in the formation of a well-defined bilayered structure of transparent fcc Co_3O_4 on top of metallic Co. Magneto-optical spectral measurements reveal strong resonance-type enhancement of the Kerr rotation and ellipticity by up to a factor of 10 compared to bulk Co. These enhancements clearly correlate with minima in the reflectivity and can be quantitatively modeled using bilayer optical stack calculations.

ACKNOWLEDGMENTS

One of the authors (B.R.) has been gratefully supported by means of the Deutsche Forschungsgemeinschaft. One of the authors (G.A.) thanks the Ministerio De Educacion y Ciencia (Spain) for financial support.

- ¹For a review, see D. Weller, W. Reim, and K. Spörl, *J. Magn. Magn. Mater.* **93**, 183 (1991); C. J. Lin, *Mater. Res. Soc. Symp. Proc.* **150**, 15 (1989); D. S. Bloomberg and G. A. N. Connell, in *Magneto-Optical Recording, Vol. II, Computer Data Storage*, edited by C. D. Mee and E. D. Daniel (McGraw-Hill, New York, 1989).
- ²K. Sato, H. Ikekame, Y. Tosaka, and S.-C. Shin, *J. Magn. Magn. Mater.* **126**, 553 (1993).
- ³E. R. Moog, J. Zak, and S. D. Bader, *J. Appl. Phys.* **69**, 4559 (1991).
- ⁴T. Katayama, Y. Suzuki, H. Awano, Y. Nishihara, and N. Koshizuka, *Phys. Rev. Lett.* **60**, 1426 (1988).
- ⁵See, e.g., D. Weller and W. Reim, *Appl. Phys. A* **49**, 599 (1989).
- ⁶W. J. M. de Jonge, P. J. H. Bloemen, and F. J. A. den Broeder, in *Ultra-thin Metallic Structures*, edited by B. Heinrich and J. A. C. Bland (Springer, Berlin, 1993), Vol. 1.
- ⁷F. J. A. den Broeder, W. Hoving, and P. J. H. Bloemen, *J. Magn. Magn. Mater.* **93**, 562 (1991).

- ⁸B. N. Engel, C. D. England, R. A. Van Leuwen, M. H. Wiedmann, and C. M. Falco, *Phys. Rev. Lett.* **67**, 1910 (1991).
- ⁹A. Bartos, D. Wiarda, Z. Inglot, K. P. Lieb, M. Uhrmacher, and T. Wenzel, *Int. J. Mod. Phys. B* **7**, 357 (1993).
- ¹⁰See, e.g., L. Smardz, U. Kobler, and W. Zinn, *Vacuum* **42**, 283 (1991); and references therein.
- ¹¹W. Reim and J. Schönes, in *Ferromagnetic Materials*, edited by E. P. Wohlfarth and K. H. J. Buschow (North-Holland, Amsterdam, 1990), Vol. 5, p. 133.
- ¹²D. Weller, *Spin-Orbit-Influenced Spectroscopy of Magnetic Solids*, Lecture Notes in Physics (Springer, Berlin, 1996), p. 466.
- ¹³P. Ruzakowski Athey, F. K. Urban III, M. F. Tabet, and W. A. McGahan, *J. Vac. Sci. Technol. A* **14**, 685 (1996).
- ¹⁴K. Balasubramanian, H. A. Mcleod, and A. S. Marathay, *Proc. SPIE* **1078**, 214 (1989).
- ¹⁵J. H. Weaver, C. Krafke, D. W. Lynch, and E. E. Koch, in: *Physics Data*, Vol. 18: *Optical Properties of Metals*, Pt. 1, edited by H. Behrens and G. Ebell (Fachinformationszentrum Energie, Physik, Mathematik GmbH, Karlsruhe, Eggenstein-Leopoldshafen 2, 1981), p. 91.